JOURNAL OF MATERIALS SCIENCE 31 (1996) 2757–2765

Sintering of magnesium oxide powder prepared by vapour-phase oxidation process – Relationship between particle size and mechanical properties of consolidated specimens

AKIRA ITOH, KIYOSHI ITATANI, F. S. HOWELL, AKIRA KISHIOKA, MAKIO KINOSHITA
Department of Chemistry, Faculty of Science and Engineering, Sophia University, 7-1 Kioi-cho, Chiyoda-ku, Tokyo 102 Japan

Relationship between powder properties and bending strengths of the sintered magnesium oxide (MgO) specimens was examined using seven kinds of MgO powders prepared by a vapour-phase oxidation process; the average primary particle sizes were 11, 25, 32, 44, 57, 107 and 261 nm. These compressed powders (specimens) were fired at 1600 or 1700 °C for 1 to 15 h. Although the densification behaviours of the specimens varied with the primary particle size of the starting powders, the relative densities of the specimens fired at 1700 °C for 5 h were all in the range of 97–98%. The relationships between bending strengths and grain sizes of these sintered specimens could be classified into two categories, according to the primary particle size of the starting powder: (i) at and below 32 nm and (ii) 44–261 nm. In range (i), the bending strengths of the sintered specimens were as low as ~ 120 MPa; the grain size was reduced from 50.7 to 35.8 μm as the primary particle size decreased from 32 to 11 nm. In range (ii), as the primary particle size increased from 44 to 261 nm, the bending strength of the sintered specimen was enhanced from 162 to 183 MPa, while the grain size was reduced from 28.3 to 13.7 μm.

1. Introduction

Since magnesium oxide (MgO) has the advantages of a high melting point (2800 °C), high electrical resistance (1×10^{17} Ω (R.T.)) and excellent resistance to alkali melts, it is now used in various fields, such as for refractories, crucibles, substrates for electronics and optical lenses [1,2]. Nevertheless, since its mechanical strength and thermal shock resistance are too low for practical uses, recent attention has been directed toward the fabrication of dense MgO ceramics from the easily sinterable MgO powder [3] and/or the reinforcement of MgO ceramics with whiskers [4] or zirconia [5–7].

The vapour-phase oxidation process is known as a novel technique for the preparation of easily sinterable MgO powder with high purity (over 99.9%), submicrometre-sized particles, narrow particle size distribution and "soft" agglomerates [8–14]. By using this powder, the dense MgO ceramics could be fabricated; moreover, the mechanical strengths (bending strength, fracture toughness and thermal shock resistance) of such dense MgO ceramics have been evaluated previously [3, 15]. Nevertheless, since the previous researchers dealt with only one or a few MgO powders as starting material(s), the relationship between powder properties and mechanical strength of MgO ceramics has never been clarified systematically.

The present authors have evaluated the sinterabilities of MgO powders prepared by the vapour-phase oxidation process [16], using seven kinds of MgO powders with different primary particle sizes ranging from 11 to 261 nm. In the next step of this research, we describe (i) the fabrication of the dense MgO ceramics obtained from these powders, (ii) the bending strength of these MgO ceramics and (iii) the relationships between relative density, grain size and bending strength of these MgO ceramics.

2. Experimental details

2.1. Starting materials

Seven kinds of MgO powders prepared by the vapour-phase oxidation process were provided by Ube Industries, Ltd. The average primary particle sizes of the MgO powders calculated on the basis of the specific surface areas were 11, 25, 32, 44, 57, 107 and 261 nm; these MgO powders were designated as A(11), B(25), C(32), D(44), E(57), F(107) and G(261), respectively [16].

2.2. Fabrication and firing of the specimens

Rectangular-shaped solid specimens with sizes of 45 mm by 5 mm by 5 mm were fabricated by pressing

0022–2461

1.5–2.0 g of MgO powder uniaxially at 30 MPa. The specimens were heated up to the desired temperature (1600 or 1700 °C) at a rate of 10 °C min^{-1} and were held there for 1 to 15 h.

2.3. Three-point bending test

The bending strengths of the sintered specimens, with sizes of 30 mm by 3.5 mm by 3 mm, were measured at room temperature, using a universal testing machine (Model YZ-500-1-PC, Yasuda Seiki Seisakusho, Tokyo). The span and crosshead speed were 25 mm and 0.5 mm min^{-1}, respectively.

2.4. Microstructural evaluation

The polished and fracture surfaces of the sintered specimens were observed using a scanning electron microscope (SEM: Model S-430, Hitachi, Tokyo). The polished surfaces, which had been etched thermally at 50 °C lower than the specimen firing temperature, were observed in order to measure the grain sizes by an intercept method [17]. The fracture surface was observed in order to elucidate the crack-propagation path.

3. Results

3.1. Relative density, grain size and microstructure

High mechanical strength cannot be achieved until most of the pores are eliminated from a specimen. Thus the firing time for the fabrication of a high-density MgO specimen was examined by fixing the firing temperature to 1600 or 1700 °C [16]. We describe the changes in relative density, grain size and bending strength during the firing of the specimens at 1600 and 1700 °C for 1 to 15 h.

3.1.1. Relative density

Fig. 1a shows the changes in relative densities during the firing of the specimen at 1600 °C; the relative densities of specimens B(25) and C(32) were omitted in this figure, because they were almost the same as those of specimen A(11). The relative densities of specimens A(11) were 96–97% for the firing time of 1 to 5 h; on further firing to 15 h, however, the relative density decreased down to ~ 95%. The relative densities of specimens D(44) and E(57) were in the range of 97–99% over the firing time of 1 to 15 h. The relative densities of specimens F(107) increased with time and attained 97.6% for 5 h; they remained unchanged during firing from 5 to 15 h. The relative densities of specimens G(261) increased with time and attained 96.5% after 15 h.

Fig. 1b shows the changes in relative densities during the firing of specimens at 1700 °C. The relative densities of specimens A(11) were 97–98% on firing for 1 to 5 h; on further firing to 15 h, however, they decreased down to 93.6%. Little change in relative densities of specimens D(44), E(57) and F(107) were observed over the firing time of 1 to 15 h. The relative densities of specimens G(261) increased with time and attained 97.4% on firing for 5 h; they remained unchanged on further firing.

3.1.2. Microstructure and grain size

Since the relative densities of specimens A(11) decreased with time from 5 to 15 h at 1600 °C, the microstructures of specimens A(11) fired at 1600 °C were examined by SEM. Typical results for the specimens fired for 5 and 15 h are shown in Fig. 2. For the firing time of 5 h (Fig. 2a), the grains with sizes of 10 to 50 μm were closely packed. On further firing to 15 h (Fig. 2b), however, the pores were present chiefly on grain boundaries.

Since the relative densities of specimens of type A(11) to G(261) fired at 1700 °C for 5 h attained

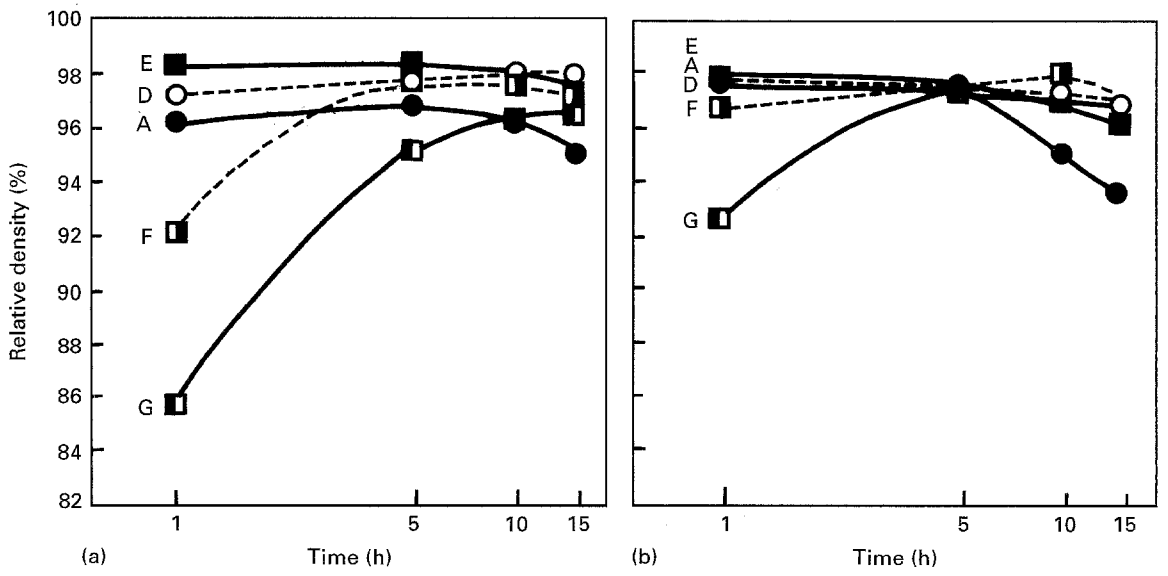

Figure 1 Effect of primary particle size on relative density of (a) specimens fired at 1600 °C and (b) specimens fired at 1700 °C. ●: A(11), ○: D(44), ■: E(57), ◨: F(107), ◧: G(261),

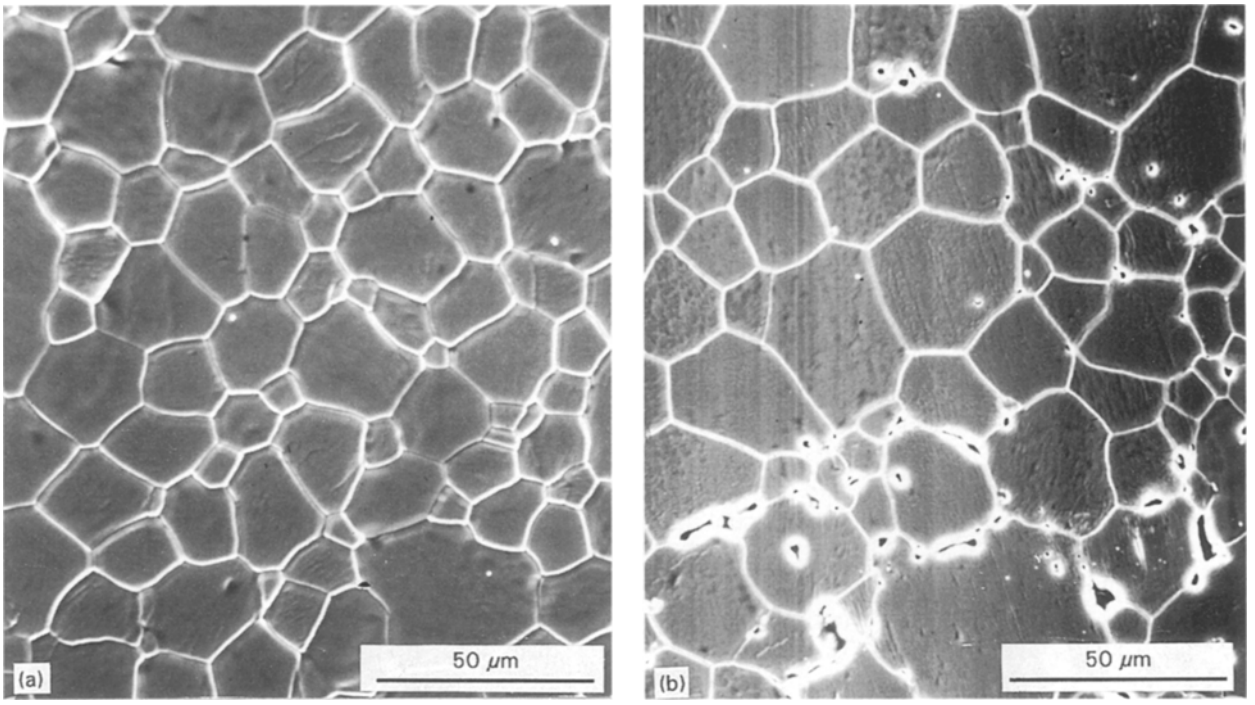

Figure 2 Typical SEM micrographs of specimens A(11) fired at 1600 °C for (a) 5 h and (b) 15 h.

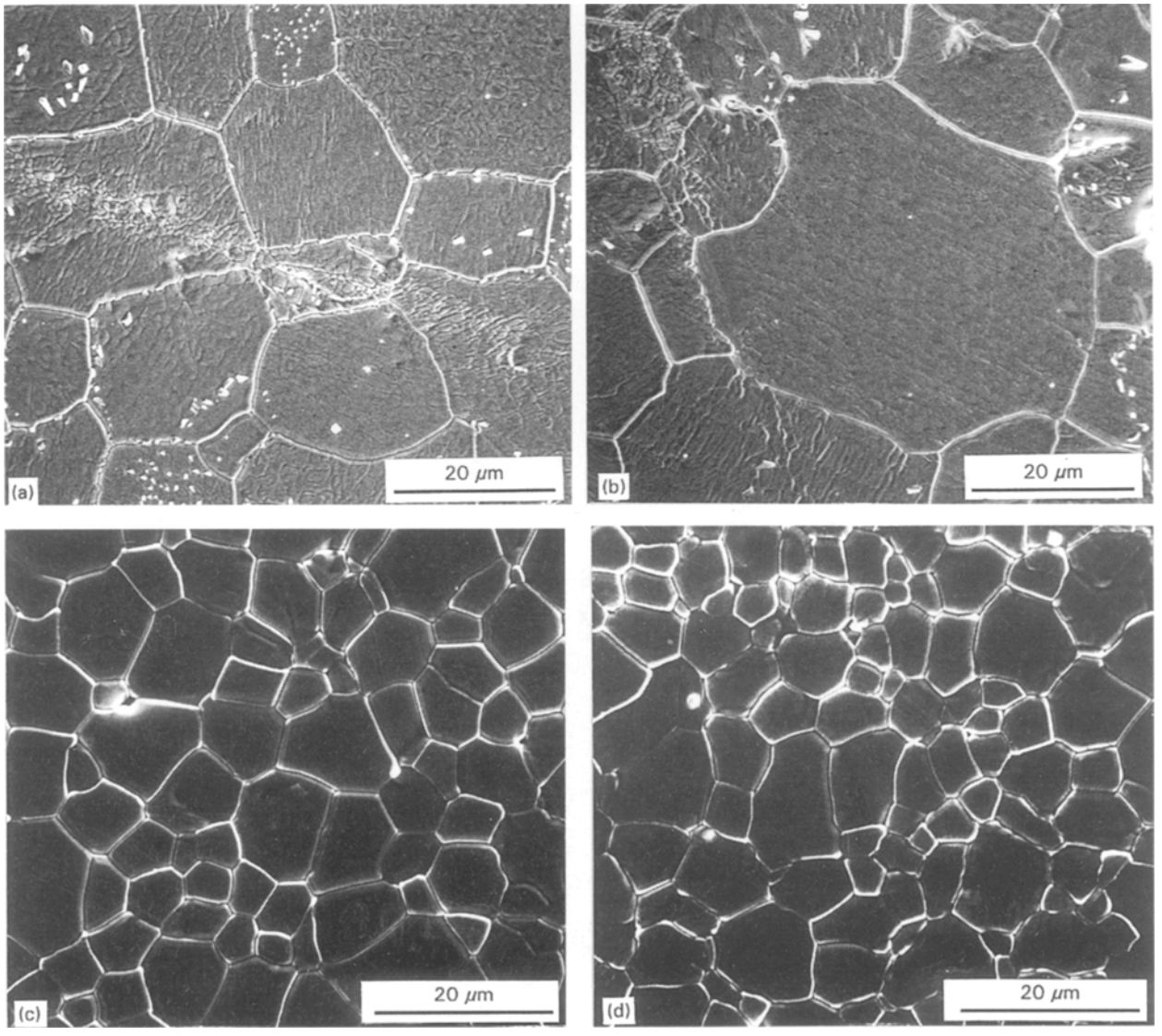

Figure 3 SEM micrographs of (a) specimen A(11), (b) specimen C(32), (c) specimen E(57) and (d) specimen G(261) fired at 1700 °C for 5 h.

around 98%, the microstructures of these specimens were observed by SEM. Typical results for specimens of type A(11), C(32), E(57) and G(261) are shown in Fig. 3. The microstructure (Fig. 3a) of specimen A(11) showed that the grains with sizes of 10–40 μm were closely packed. The microstructure (Fig. 3b) of specimen C(32) revealed that the grain sizes were 20–60 μm and were larger than those of specimen A(11). The microstructures (Fig. 3c and d) of specimens E(57) and G(261) showed that the grain sizes were reduced with increasing primary particle size.

On the basis of SEM observation, the logarithms of the average grain sizes were plotted against the firing time. Results of the specimens fired at 1600 °C are shown in Fig. 4a. The relationship between grain size and firing time of each specimen was expressed as a straight line. The magnitudes of these grain sizes over the firing times of 1 to 15 h were arranged as follows: specimen C(32) > specimen B(25) > specimen A(11) > specimen D(44) > specimen E(57) > specimen F(107) > specimen G(261).

The changes in grain sizes during the firing of specimens at 1700 °C are shown in Fig. 4b. The grain sizes of the specimens increased with time. The relationship between the logarithm of grain size and time of each specimen was again expressed as a straight line. The magnitudes of the grain sizes follow the same sequence as those fired at 1600 °C.

3.2. Bending strength

As shown in Section 3.1, the decreases in relative densities for specimens A(11)–C(32) were observed when the firing time exceeded 5 h; thus the bending strengths were measured only after the specimens were fired for 5 h at 1600 or 1700 °C. Details are described in this section.

3.2.1. Specimens fired at 1600 °C for 5 h

The relative densities, grain sizes and bending strengths of the sintered specimens are plotted against the primary particle sizes of the starting powders. Results are shown in Fig. 5. The relative density became a maximum (98.0%) when the primary particle size was 54 nm; however, it decreased down to 95.2% as the primary particle size increased up to 261 nm. The average grain size became a maximum (38.7 μm) when the primary particle size was 32 nm; it decreased down to 5.9 μm with increasing primary particle size up to 261 nm. The bending strength increased with increasing primary particle size and exhibited a maximum (175 MPa) for a primary particle size of 54 nm; it decreased down to 140 MPa with further increases in the primary particle size.

The fracture surfaces of the sintered specimens were observed by SEM. Typical results are shown in Fig. 6. The fracture surfaces of specimens A(11) and C(32) (Fig. 6a and b) showed that the cracks propagated along the cleavage planes (see the fractured grains; transgranular fracture). The fracture surface (Fig. 6c) of specimen E(57) showed that the cracks propagated not only through the transgranular region but also through the intergranular region. The fracture surface (Fig. 6d) of specimen G(261) revealed that most of the cracks propagated through the intergranular region, because the appearance of the original grains remained unchanged.

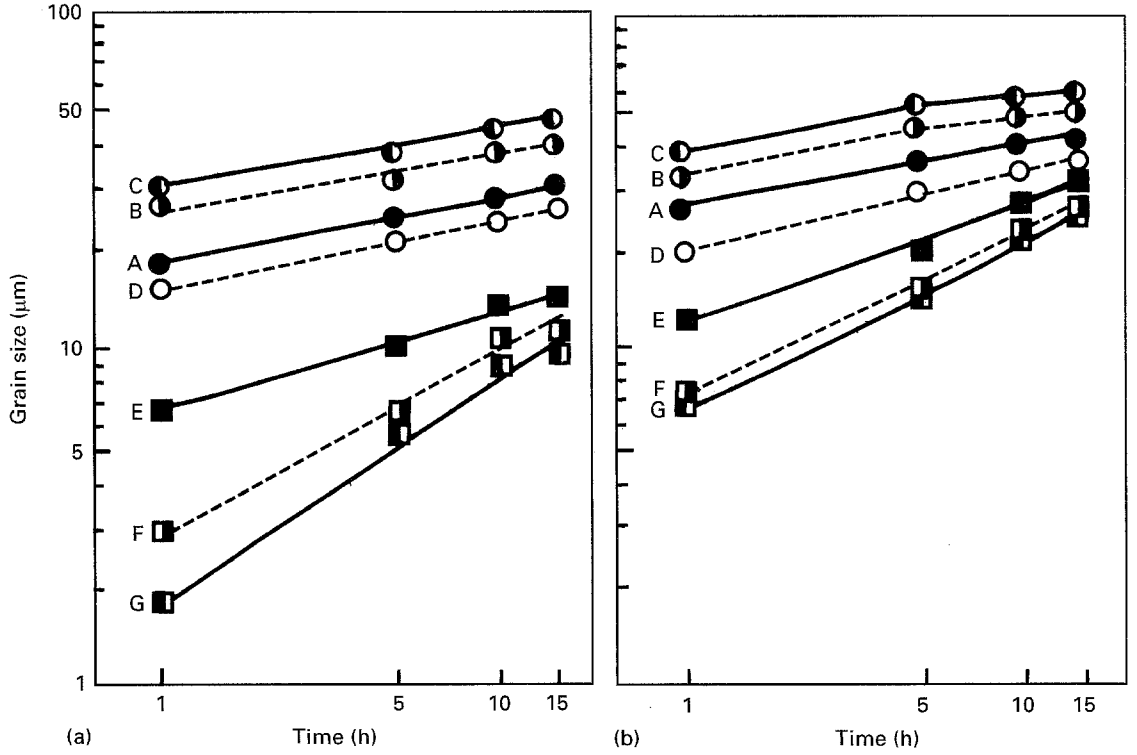

Figure 4 Changes in grain sizes during the firing of specimens at (a) 1600 °C and (b) 1700 °C. ●: A(11), ◑: B(25), ◐: C(32), ○: D(44), ■: E(57), ◨: F(107), ◧: G(261).

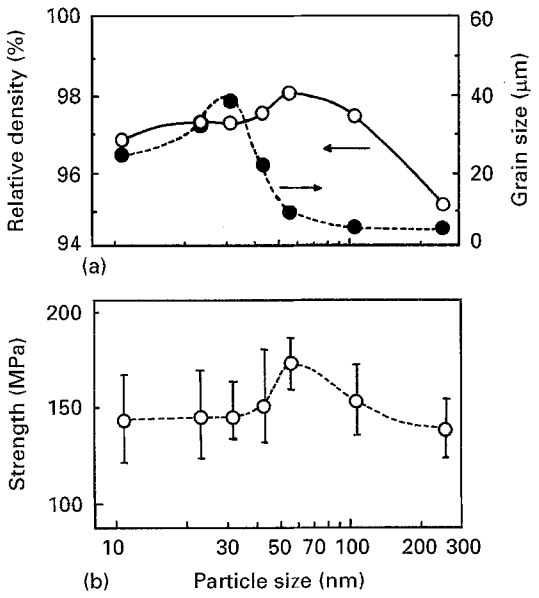

Figure 5 Effect of primary particle size on (a) relative density (○) and grain size (●) and (b) bending strength of the specimen fired at 1600 °C for 5 h.

3.2.2. Specimens fired at 1700 °C for 5 h

The bending strengths of the sintered specimens are shown in Fig. 7, together with the relative densities and grain sizes. The relative densities of these specimens were in the range of 97 to 98%. The grain size became a maximum (50.7 μm) when the primary particle size was 32 nm; however, the grain size decreased with increasing primary particle size and became 13.7 μm when the primary particle size was 261 nm. The bending strengths were ~ 120 MPa for primary particle sizes below 32 nm; they increased with increasing primary particle size and attained ~ 180 MPa at 107 nm or larger primary particle size.

The fracture surfaces of typical sintered specimens are shown in Fig. 8. The fracture surfaces (Fig. 8a to c) of specimens A(11), F(107) and C(32) showed that most of the cracks propagated through the transgranular region. The fracture surface (Fig. 8d) of specimen G(261) revealed that the cracks propagated not only through the transgranular region but also through the intergranular region.

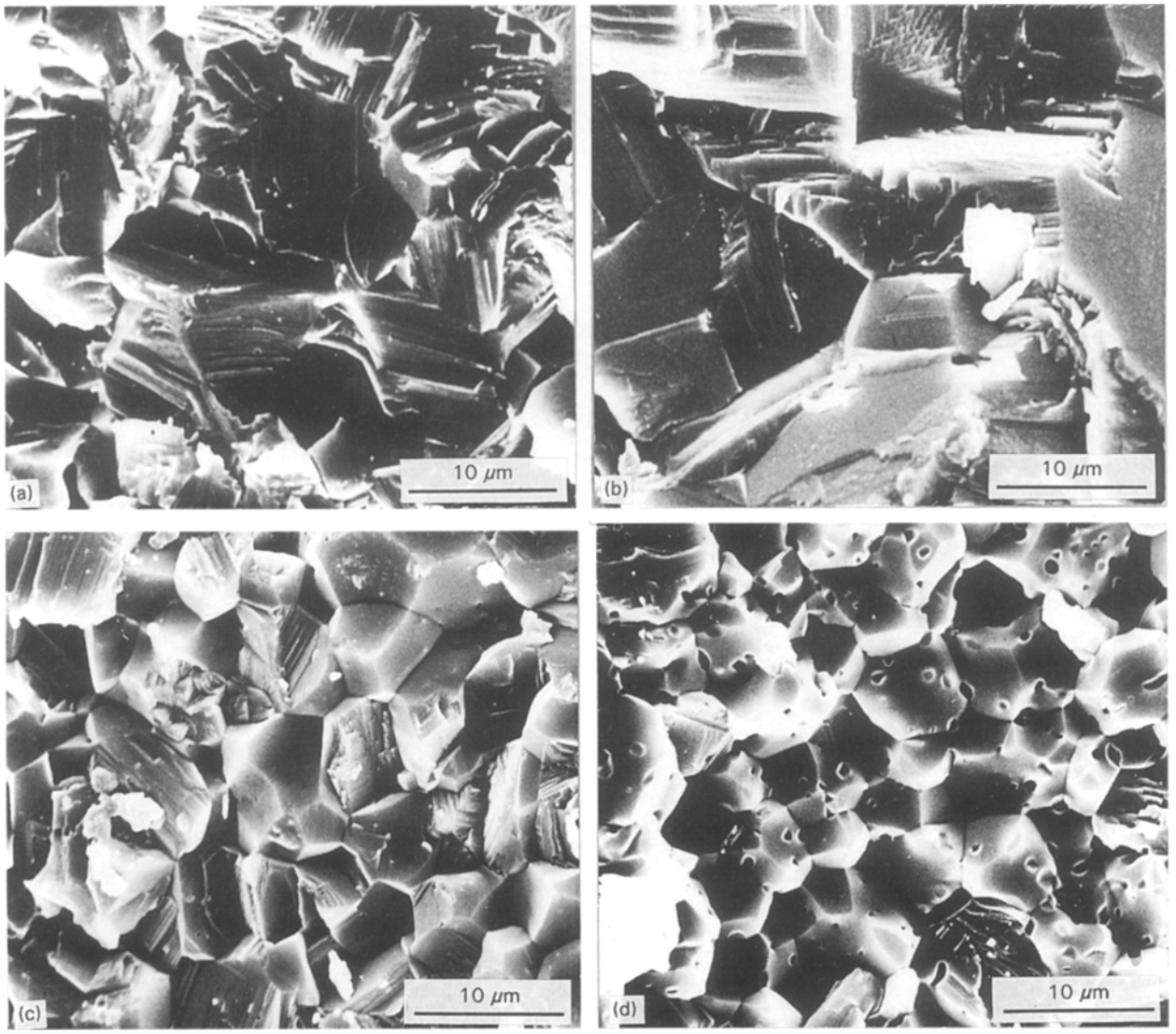

Figure 6 Typical SEM micrographs of the fracture surfaces of (a) specimen A(11), (b) specimen C(32), (c) specimen E(57) and (d) specimen G(261) fired at 1600 °C for 5 h

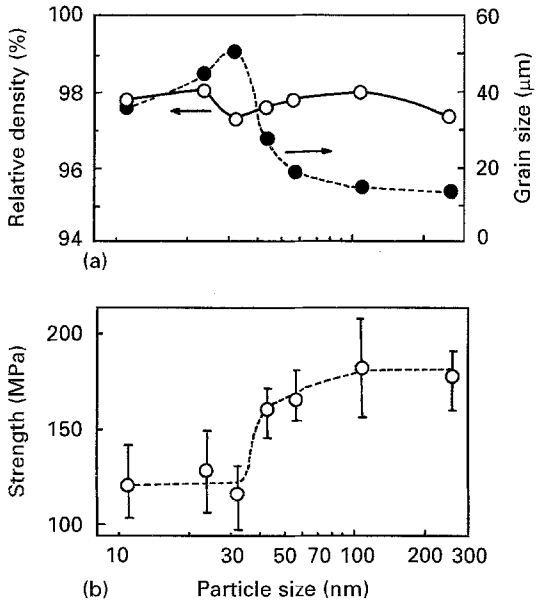

Figure 7 Effect of primary particle size on (a) relative density (○) and grain size (●) and (b) bending strength of the specimen fired at 1700 °C for 5 h.

4. Discussion

The changes in relative densities, microstructures and bending strengths during the firing of the specimens at 1600 and 1700 °C are classified into two categories, according to the primary particle size of the starting powder: (i) at and below 32 nm and (ii) 44–261 nm. Taking this classification into account, we describe the properties of the sintered specimens in this section.

4.1. Changes in relative densities during firing

Although the relative densities of specimens of type A(11)–C(32) fired at 1600 and 1700 °C are in the range of 96–98% during firing for 1 to 5 h, they are reduced on further firing (Fig. 1a and b). The SEM observations of these sintered specimens show that pores are created when the firing time exceeds 5 h and that the number of these pores increases with firing temperature (Fig. 2). Thus the decrease in relative density can be attributed to the creation of pores. These pores may be created after residual H_2O/CO_2 molecules, which have dissolved into the grains, are

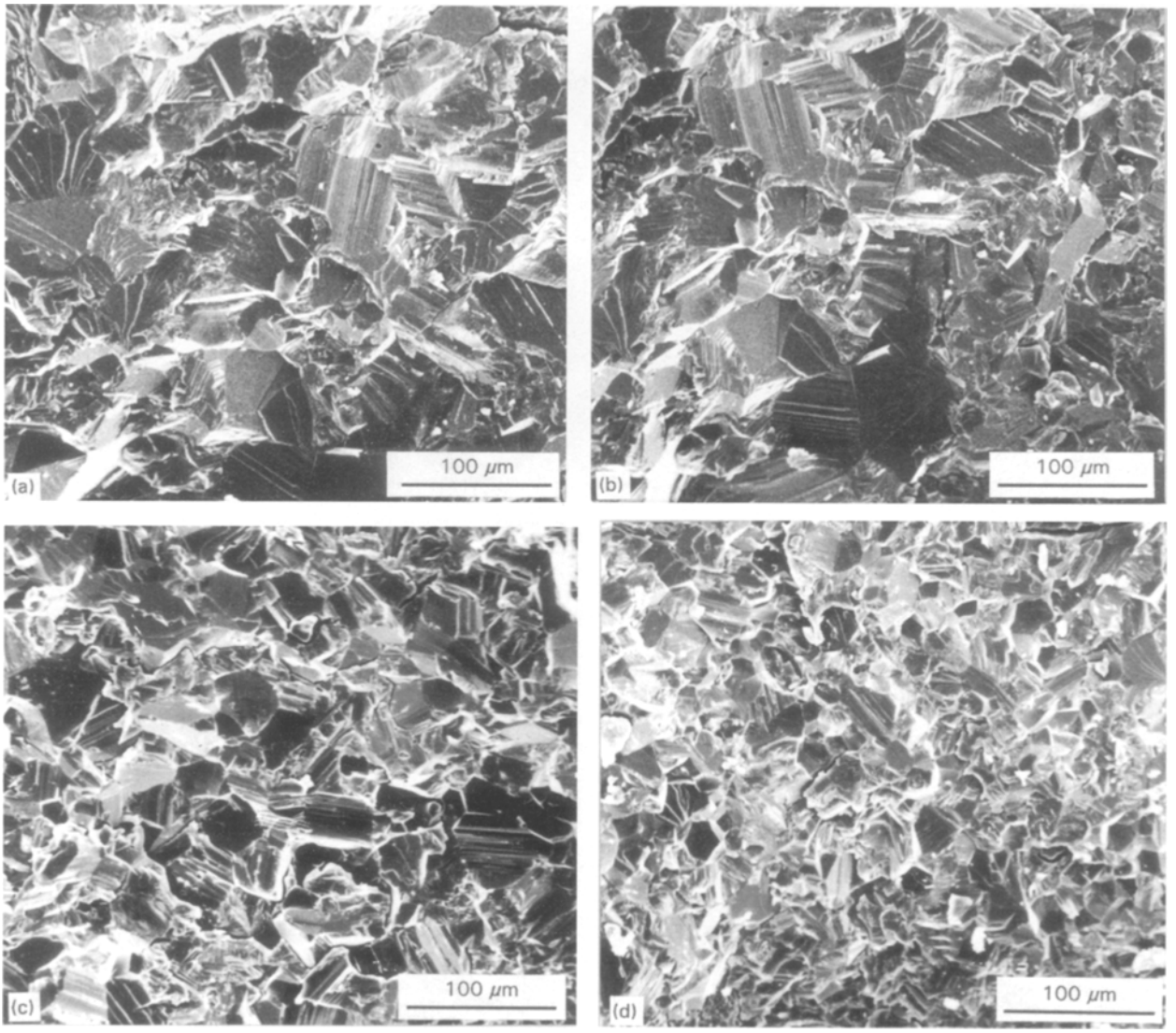

Figure 8 Typical SEM micrographs of the fracture surfaces of (a) specimen A(11), (b) specimen C(32), (c) specimen E(57) and (d) specimen G(261) fired at 1700 °C for 5 h.

released from the specimens [12, 18, 19], because the amount of H_2O/CO_2 molecules adsorbed on MgO particles increases with decreasing primary particle size.

Little changes in relative densities (97–99%) of specimens of type D(44) and E(57) are observed over firing times of 1 to 15 h at 1600 or 1700 °C (Fig. 1a and b), because the amount of residual H_2O/CO_2 molecules is much smaller than for specimens of type A(11)–C(32). This phenomenon may be supported by the fact that the weight losses (1–2%) of specimens of type D(44) and E(57) fired at these temperatures were smaller than those (~ 10%) for specimens of type A(11)–C(32).

The relative densities of F(107) and G(261) specimens at 1600 °C are enhanced during firing from 5 to 10 h and become almost constant (96–98%) on further firing (Fig. 1a). When the firing temperature is raised to 1700 °C, the relative density of specimen F(107) attains ~ 97% only when firing for 1 h; however, the relative density of specimen G(261) does not exceed 96% until the firing time is extended to 5 h. These results indicate that the densification of specimen G(261) is retarded more than that of specimen F(107), reflecting the difference in the primary particle size (Fig. 1b).

4.2. Changes in grain sizes during the firing

The relationship between grain size (d) and firing time (t) is expressed as follows [20]:

$$d^n - d_0^n = kt \quad (1)$$

where n and k represent constants and d_0 is the grain size at $t = 0$. Since the grain sizes of the pure MgO ceramics generally follow the square growth law [21–26], we incorporated our data into Equation 1 by assuming the value of n to be 2. The logarithmic relationship between ($d^2 - d_0^2$) and time (t) for specimens A(11)–G(261) fired at 1700 °C for 1 to 5 h are shown in Fig. 9. The plots for these specimens were expressed as straight lines with a slope near unity, specimens except for A(11)–C(32) fired for 5 h or longer.

As shown above, the present data follow the square growth law, except for the cases of specimens A(11)–C(32) fired for 5 h or longer. The fitting of the data to the square growth law indicates that the pore migration which controls the grain-boundary motion or grain growth may be preceded by vapour transport, i.e. the evaporation/condensation of material within the pores [20]. The deviation of the slope from unity, which is observed for specimens A(11)–C(32) fired for 5 h or longer, is attributed to the creation of pores during the firing (Fig. 2b).

The grain size decreases as the primary particle size decreases from 32 to 11 nm (Figs 3, 4, 5 and 7). This phenomenon is contrary to what we had expected: grain growth should be promoted with decreasing primary particle size, because smaller particles have higher surface energies which act as a driving force in sintering: however, since the number of pores created during firing increases when primary particle size decreases, the grain growth may be retarded due to the creation of these pores. On the other hand, the grain size decreases as primary particle size increases from 44 to 261 nm (Figs 3, 4, 5 and 7), which suggests that the grain growth as well as the densification of the specimen may be slowed down when the primary particle size increases.

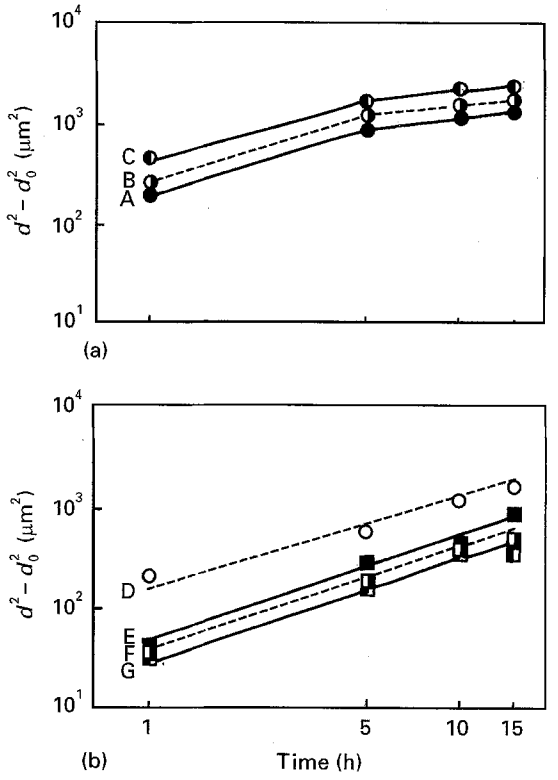

Figure 9 Logarithmic relationship between ($d^2 - d_0^2$) and time for specimens A(11)–G(261) fired at 1700 °C. d: Grain size at time = t, d_0: Grain size at $t = 0$, ●: A(11), ◑: B(25), ◐:C(32), ○: D(44), ■: E(57), ◨: F(107), ◧: G(261).

4.3. Bending strength of the sintered specimen

The bending strengths of specimens A(11)–C(32) fired at 1600 °C for 5 h are ~ 140 MPa (Fig. 5). Although the relative densities of these sintered specimens rose slightly from ~ 97% to ~ 98% with firing temperature from 1600 to 1700 °C, the bending strengths of the specimens fired at 1700 °C for 5 h are reduced to ~ 120 MPa (Fig. 7). Such reduction of the bending strengths may be attributed to the increases in grain sizes with firing temperature from 1600 to 1700 °C (Figs 2a, 3a and 4) [27].

The bending strength of specimen E(57) is the highest (175 MPa) among the specimens (Fig. 5) fired at 1600 °C for 5 h, this may result from the low porosity (1.5%) and small grain size (10.3 μm). On the other hand, the bending strength of specimen G(261) fired at 1600 °C for 5 h is as low as 140 MPa (Fig. 5), partly because the relative density is only 95.2% and partly because the pores are located not within grains but on grain boundaries (Fig. 6d) [27]. The relative density of specimen G(261), however, increases up to ~ 98% and the bending strength is enhanced up to 183 MPa when the firing temperature is raised up to 1700 °C (Fig. 7).

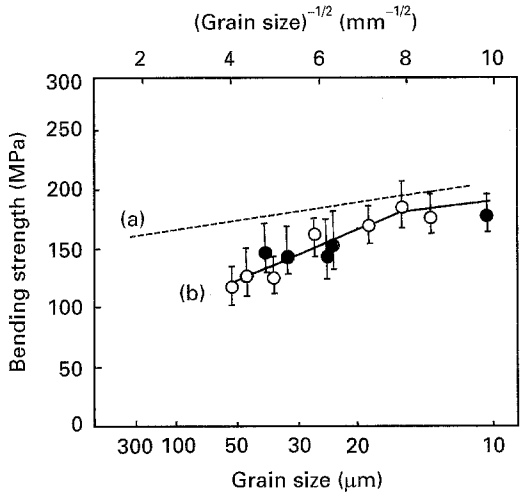

Figure 10 Relationship between bending strength and grain size. (a) Data on hot-pressed specimens reported by Yasuda *et al.* [15]. (b) The present data, ●: 1600°C, ○: 1700°C.

Yasuda *et al.* [15] hot pressed the MgO powders prepared by the vapour-phase oxidation process and measured the bending strengths of the high-density sintered MgO specimens; they found that the relationship between bending strength (σ) and grain size (d) follows the Petch equation [28]:

$$\sigma = a + bd^{-\frac{1}{2}} \quad (2)$$

where a and b are constants.

The Petch equation is valid when the grain sizes of MgO specimens are below $\sim 60\,\mu m$ [28]. On the basis of Equation 2, the bending strengths of the specimens fired at 1600 and 1700 °C for 5 h are plotted against $d^{-\frac{1}{2}}$. The results are shown in Fig. 10, together with the data on hot-pressed MgO specimens [15]. The relationship between relative density and grain size is expressed as two straight lines with the break point at a grain size of 15 μm. The bending strength increases with decreasing grain size. At grain sizes of 15 μm or smaller, little difference in the bending strengths is observed between the present and hot-pressed specimens. The bending strength of the present MgO specimen is estimated to be ~ 180 MPa with a grain size of 10 μm.

The crack-propagation path changes from intergranular (Fig. 6d) to transgranular (Fig. 6a–c and Fig. 8a–d) when the grain size exceeds $\sim 20\,\mu m$. This fact may be confirmed by Shiono *et al.* [29], who found that the fracture path changes from intergranular to transgranular when the grains have grown to be 1–10 μm or larger.

5. Conclusion

The relationship between powder properties and bending strengths of the sintered magnesium oxide (MgO) specimens was examined using seven kinds of MgO powders prepared by the vapour-phase oxidation process; the primary particle sizes were in the range of 11 to 261 nm. The results are summarized as follows:

1. When the compressed powders (specimens) were fired at 1600 or 1700 °C for 5 h, the relative densities were in the range of 96–98%. On prolonged firing, the relative densities of the specimens derived from the powders with primary particle sizes of 11–32 nm decreased down to $\sim 94\%$, because pores were created when residual H_2O/CO_2 molecules, which had dissolved into the grains, were released from the specimen during firing.
2. The relationships between relative density, grain size and bending strength of specimens fired at 1700 °C for 5 h could be classified into two categories, according to the primary particle size. In region (i), at and below 32 nm, the bending strengths of the sintered specimens were as low as ~ 120 MPa; the grain size was reduced from 50.7 to 35.8 μm as the primary particle size decreased from 32 to 11 nm. In region (ii), 44–261 nm, as the primary particle size increased from 44 to 261 nm, the bending strength of the sintered specimen was enhanced from 162 to 183 MPa, while the grain size was reduced from 28.3 to 13.7 μm.

Acknowledgements

The authors wish to express their thanks to Ube Industries Ltd. for providing the sample powders.

References

1. K. YAMAMOTO, *Bull. Ceram. Soc. Jpn.* **15** (1980) 176.
2. Y. TAKAMIYA, *ibid.* **17** (1982) 823.
3. A. NISHIDA, T. SHIMAMURA and Y. KOHTOKU, *J. Ceram. Soc. Jpn.* **98** (1990) 412.
4. T. NISHIDA, T. SHIONO, H. YAMAUCHI and T. NISHIKAWA, *J. Soc. Mater. Sci. Jpn.* **36** (1987) 17.
5. T. OKAMOTO, Y. IKUMA, M. SHIMAOKA, T. SHIROTORI and W. KOMATSU, *J. Ceram. Soc. Jpn.* **97** (1989) 812.
6. A. NISHIDA, M. FUKUDA, Y. KOHTOKU and K. TERAI, *ibid.* **100** (1992) 191.
7. A. NISHIDA and K. TERAI, *ibid.* **100** (1992) 1113.
8. T. WATARI, K. NAKAYOSHI and A. KATO, *Nippon Kagaku Kaishi* **1984** (1984) 1075.
9. A. KATO, *Ind. Ceram.* 7 (1987) 105.
10. A. NISHIDA, A. UEKI and K. YOSHIDA, in "Advances in Ceramics: Ceramic Powder Science", Vol. 21, edited by G. L. Messing, K. S. Mazdiyasni, J. W. McCauley and R. A. Haber (The American Ceramic Society, Westerville, OH, 1987) p. 265.
11. A. NISHIDA, A. UEKI and K. YOSHIDA, in "Advances in Ceramics: Ceramic Powder Science", Vol. 21, edited by G. L. Messing, K. S. Mazdiyasni, J. W. McCauley and R. A. Haber (The American Ceramic Society, Westerville, OH, 1987) p. 271.
12. T. WATARI, K. NAKAYOSHI and K. KATO, *Nippon Kagaku Kaishi* **1985** (1985) 790.
13. K. ITATANI, M. NOMURA, A. KISHIOKA and M. KINOSHITA, *J. Mater. Sci.* **21** (1986) 1429.
14. A. NISHIDA, T. SHIMAMURA and Y. KOHTOKU, *J. Ceram. Soc. Jpn.* **97** (1989) 107.
15. K. YASUDA, S.-D. KIM, Y. KANEMICHI, Y. MATSUO and S. KIMURA, *ibid.* **98** (1990) 1103.
16. K. ITATANI, A. ITOH, F. S. HOWELL, A. KISHIOKA and M. KINOSHITA, *J. Mater. Sci.* **28** (1993) 719.
17. R. L. FULLMAN, *Trans. AIME* **197** (1953) 447.
18. R. L. COBLE, *J. Amer. Ceram. Soc.* **45** (1962) 123.
19. O. YAMAGUCHI, H. TONAMI and K. SHIMIZU, *Chem. Lett.* **1976** (1976) 799.
20. R. J. BROOK, in "Treatises on Materials Science and Technology: Ceramic Fabrication Process", Vol. 9, edited by F. F. Lange and Y. Wang (Academic Press, New York, 1976) p. 331.

21. A. U. DANIELS, JR., R.C. LOWRIE, JR., R. L. GIBBY and I. B. CUTLER, *J. Amer. Ceram. Soc.* **45** (1962) 282.
22. R. M. SPRIGGS, L. A. BRISSETTE and T. VASILOS, *ibid.* **47** (1964) 417.
23. R. S. GORDON, D. D. MARCHANT, G. W. HOLLENBERG, *ibid.* **53** (1970) 399.
24. C. M. KAPADIA and M. H. LEIPOLD, *ibid.* **57** (1974) 41.
25. O. YAMAGUCHI, H. TONAMI, T. HAYASHI and K. SHIMIZU, *J. Jpn. Soc. Powder Powder Metall.* **24** (1977) 157.
26. J. D. HODGE and R. S. GORDON, *Ceram. Int.* **4** (1978) 17.
27. R. W. RICE, *Proc. Br. Ceram. Soc.* **20** (1972) 329.
28. S. C. CARNIGLIA, *J. Amer. Ceram. Soc.* **48** (1965) 580.
29. T. SHIONO, H. NOZAWA, T. NISHIDA and Y. NISHIKAWA, in Proceedings of Annual Meeting of the Ceramic Society of Japan, Tokyo, May 1988 (The Ceramic Society of Japan, Tokyo, 1988) p. 107.

Received 10 March
and accepted 8 September 1995